Subcellular distribution of chelatable iron: a laser scanning microscopic study in isolated hepatocytes and liver endothelial cells

Frank PETRAT, Herbert DE GROOT and Ursula RAUEN[1]

Institut für Physiologische Chemie, Universitätsklinikum, Hufelandstrasse 55, D-45122 Essen, Germany

The pool of cellular chelatable iron ('free iron', 'low-molecular-weight iron', the 'labile iron pool') is usually considered to reside mainly within the cytosol. For the present study we adapted our previously established Phen Green method, based on quantitative laser scanning microscopy, to examine the subcellular distribution of chelatable iron in single intact cells for the first time. These measurements, performed in isolated rat hepatocytes and rat liver endothelial cells, showed considerable concentrations of chelatable iron, not only in the cytosol but also in several other subcellular compartments. In isolated rat hepatocytes we determined a chelatable iron concentration of 5.8 ± 2.6 μM within the cytosol and of at least 4.8 μM in mitochondria. The hepatocellular nucleus contained chelatable iron at the surprisingly high concentration of 6.6 ± 2.9 μM. In rat liver endothelial cells, the concentration of chelatable iron within all these compartments was even higher (cytosol, 7.3 ± 2.6 μM; nucleus, 11.8 ± 3.9 μM; mitochondria, 9.2 ± 2.7 μM); in addition, chelatable iron (approx. 16 ± 4 μM) was detected in a small subpopulation of the endosomal/lysosomal apparatus. Hence there is an uneven distribution of subcellular chelatable iron, a fact that is important to consider for (patho)physiological processes and that also has implications for the use of iron chelators to inhibit oxidative stress.

Key words: iron chelators, mitochondria, nucleus, Phen Green, transition-metal ions.

INTRODUCTION

Iron is a ubiquitous metal in cells, present in the structure of many enzymes and proteins [1] and therefore essential for life. However, iron has an enormous damaging potential: a small 'transit' pool of cellular iron is believed to catalyse the generation of highly reactive oxygen species within mammalian cells. This 'transit' pool links the cellular iron uptake via transferrin with the iron storage in proteins (i.e. ferritin) and the synthesis of iron-containing proteins (haem and non-haem iron proteins [2,3]). Iron belonging to this 'transit' pool is thought to be in a steady-state equilibrium, bound to low-molecular-weight compounds (such as ATP, citrate or phosphate) or loosely attached to proteins [2]; it can be defined as 'chelatable' because chelating molecules can be used for its detection.

Cellular chelatable iron is generally referred to as being cytosolic [2–5], although there is also evidence for the existence of chelatable iron in other metabolic compartments of the cell. In mitochondria, for example, iron is incorporated into protoporphyrin IX during haem synthesis. A 'transit' pool of chelatable iron must therefore be assumed to exist within these organelles; attempts to measure it have been made with isolated mitochondria [6–9]. Some attention has also been given to redox-active iron within lysosomes [10,11], which has been shown to be responsible for oxidative cell injury under different pathological conditions [12–14]. There are also pointers to the existence of chelatable, redox-active iron within mammalian nuclei: iron-dependent hydroxyl-radical-mediated DNA damage is reported to occur under several pathological conditions [1,2] and because the hydroxyl radical is known to react site-specifically [2], intranuclear, DNA-associated chelatable Fe^{2+} would have to be present.

Although it was first suggested several decades ago that chelatable iron probably exists within some of these subcellular compartments, the size and chemical nature of these pools have generally resisted investigation in vital cells owing to several methodological difficulties. We recently introduced a method based on digital fluorescence microscopy [15], subsequently adapted to laser scanning microscopy [16], which makes it possible to determine the concentration of chelatable iron in single intact cells. This method is based on quenching the fluorescent transition-metal indicator Phen Green SK (PG SK) by intracellular chelatable iron, and then 'dequenching' its fluorescence by adding strong membrane-permeant iron chelators [2,2′-dipyridyl (2,2′-DPD) or 1,10-phenanthroline] in excess. We have established an *ex situ* calibration method that makes it possible to determine the concentration of chelatable iron directly from changes in absolute cellular fluorescence [16]. With the high spatial resolution of laser scanning microscopy, this method should have the potential to study the subcellular distribution of chelatable iron. Our aim in the present study was therefore to determine the concentration of chelatable iron within intracellular compartments such as mitochondria, lysosomes or the nucleus in single vital cells.

EXPERIMENTAL

Animals

Male Wistar rats (200–350 g) were obtained from the Zentrales Tierlaboratorium (Universitätsklinikum, Essen, Germany). Animals were kept under standard conditions with free access to food and water. All animals received humane care in compliance with the institutional guidelines.

Abbreviations used: 2,2′-DPD, 2,2′-dipyridyl; HBSS, Hanks balanced salt solution; PG SK, Phen Green SK; TMRM, tetramethylrhodamine methyl ester.

[1] To whom correspondence should be addressed (e-mail ursula.rauen@uni-essen.de).

Materials

Leibovitz L-15 medium and RPMI 1640 medium were obtained from Gibco (Eggenstein, Germany); collagenase (HEP plus), collagen (Type R), dexamethasone, BSA and gentamicin were from Serva (Heidelberg, Germany); and DMSO, Acridine Orange and citric acid trisodium salt (dihydrate) were from Merck (Darmstadt, Germany). Fetal calf serum, 2,2′-DPD and propidium iodide were obtained from Sigma (Deisenhofen, Germany). 1,10-Phenanthroline came from Sigma–Aldrich (Steinheim, Germany), Sudan II from EGA-Chemie (Steinheim/Albuch, Germany) and digitonin from Fluka (Neu-Ulm, Germany). EDTA disodium salt was from Roche Molecular Biochemicals (Mannheim, Germany). Falcon cell culture flasks were obtained from Becton Dickinson (Heidelberg, Germany), glass coverslips were from Assistent (Sondheim/Röhn, Germany) and centrifuge tubes came from Nunc (Wiesbaden, Germany); these tubes were chosen because they generated only low contamination with iron. The fluorescent dyes PG SK (dipotassium salt) and its diacetate, and tetramethylrhodamine methyl ester (TMRM) were purchased from Molecular Probes Europe BV (Leiden, The Netherlands).

Cell culture

Hepatocytes were isolated from male Wistar rats as described previously [17]. For fluorescence measurements, 1.7×10^5 cells/cm² were seeded on collagen-coated 6.2 cm² glass coverslips in Petri dishes and cultured as described [15]. A rat liver endothelial cell line, derived from the liver of a male Wistar rat, was used for additional experiments. The cells had been isolated and cultured on glass coverslips as described previously [18,19].

Determination of intracellular chelatable iron by laser scanning microscopy

Experiments with hepatocytes were started 20–24 h after isolation of the cells. Liver endothelial cells were used for experiments on day 2 after subcultivation (the widely spread subconfluent cells allowed the best observation of the subcellular structures). Cells were loaded with PG SK (20 μM) for 10 min (hepatocytes) or 30 min (endothelial cells) at 37 °C in Hanks balanced salt solution (HBSS; 137 mM NaCl/5.4 mM KCl/1 mM $CaCl_2$/0.5 mM $MgCl_2$/0.4 mM KH_2PO_4/0.4 mM $MgSO_4$/0.3 mM Na_2HPO_4/25 mM Hepes, pH 7.4) as described previously [15] and then covered with Krebs–Henseleit buffer [115 mM NaCl/25 mM $NaHCO_3$/5.9 mM KCl/1.2 mM $MgCl_2$/1.2 mM NaH_2PO_4/1.2 mM Na_2SO_4/2.5 mM $CaCl_2$/20 mM Hepes (pH 7.4)].

A laser scanning microscope (LSM 510; Zeiss, Oberkochen, Germany) equipped with an argon laser and a helium/neon laser was used to perform the fluorescence measurements. The objective lens was a 63× (numerical aperture 1.25) Plan-Neofluar or a 63× (numerical aperture 1.40) Plan-Apochromat. The green fluorescence of PG SK excited at 488 nm using the argon laser at a power rating of 6.75 mW was collected through a 505 nm long-pass filter. Qualitative fluorescence measurements were performed with different parameters; for quantitative fluorescence microscopy we used the scanning parameters given in [16], except for some minor modifications such as higher zoom factors. In brief, confocal images (scanning time 7.8 s) were collected at 5 min intervals with the power of the argon laser set at 0.1 %. Single-cell fluorescence was determined by confining the regions of interest manually to individual cells, and subcellular fluorescence by confining them to particular cellular compartments (some cases of very dark images required electronic brightening of the images for proper positioning of these regions). Image processing and evaluation were performed with the 'physiology evaluation' software of the LSM 510 imaging system.

After establishing baseline fluorescence, cellular chelatable iron was removed from PG SK by adding the cell-permeant iron chelators 2,2′-DPD (5 mM) or 1,10-phenanthroline (1–5 mM) to the supernatant [15]. At the end of the experimental procedures the uptake of the vital dye propidium iodide was routinely determined to detect the loss of cell viability. The red fluorescence of propidium iodide excited at 543 nm using the helium/neon laser was collected through a 560 nm long-pass filter. Neither loading the cells with PG SK nor laser exposure with the settings given above had any cytotoxic effect.

Calibration *ex situ*: determination of subcellular PG SK concentrations and calibration of Fe^{2+}-induced quenching of PG SK fluorescence

Subcellular concentrations of PG SK in hepatocytes and endothelial cells were determined from the fluorescence (in arbitrary units) within the cellular compartments after 'dequenching' with 1,10-phenanthroline (1–2 mM) compared with that of PG SK (5–50 μM) standards (free dye) as described in [16]. In a cell-free system the quenching effect of Fe^{2+} on PG SK fluorescence in a 'cytosolic' medium (37 °C) was determined with the LSM 510 imaging system as reported in [16].

Controls

In control experiments, aliquots of PG SK diacetate (20 μM) in HBSS (37 °C) were supplemented with the hydrophilic, almost membrane-impermeant [15], Fe^{3+} chelator diethylenetriamine-penta-acetic acid (200 μM) or were pre-complexed to Fe^{2+} (10 μM) added from a concentrated stock solution of ferrous ammonium sulphate/citric acid trisodium salt dihydrate [16] before its addition to the cells. In other experiments, cells were preincubated with the lipophilic Fe^{2+} chelator 2,2′-DPD (5 mM) for 20 min before loading with PG SK was started (in the presence of 2,2′-DPD).

Hepatocellular fat droplets were identified by labelling with Sudan II. A saturated ethanolic Sudan II stock solution was prepared as described for Sudan III [20]. Hepatocytes were incubated for 30 min in a diluted (1:3.75, v/v) Sudan II solution at 37 °C, then washed twice with HBSS and covered with Krebs–Henseleit buffer. Sudan II fluorescence was detected with $\lambda_{excitation} = 488$ nm and $\lambda_{emission} \geqslant 505$ nm. Liver cell lysosomes were stained by the addition of Acridine Orange (0.5 μg/ml for 5–10 min at 37 °C) subsequent to measurements performed with PG SK; Acridine Orange fluorescence was detected with $\lambda_{excitation} = 488$ nm and $\lambda_{emission} \geqslant 560$ nm (with a detector gain far below that used for PG SK measurements).

Mitochondrial chelatable iron of permeabilized hepatocytes

PG SK-loaded hepatocytes were washed twice with a mitochondrial incubation medium {100 mM KCl/75 mM mannitol/25 mM sucrose/15 mM Tris/HCl (pH 7.4), i.e. as in [21] but without EDTA}, covered with 4 ml of this medium and immediately permeabilized by the addition of digitonin at a final concentration of 50–100 μM [22], which did not influence the mitochondrial membrane potential. After 10 min the permeabilized cells were washed twice with digitonin-free incubation medium (37 °C) and the fluorescence measurements were started. Changes in mitochondrial PG SK fluorescence after the addition of 1,10-phenanthroline (1–2 mM) were recorded at

5 min intervals with the excitation power of the argon laser set at 1.0 %.

Identification of mitochondria and recording of the mitochondrial membrane potential

Mitochondria were identified and their functional integrity was confirmed by membrane-potential-dependent staining with TMRM. Cells were loaded with TMRM (0.5–1 μM) for 10 min at 37 °C in HBSS, washed twice with dye-free HBSS and further incubated in Krebs–Henseleit buffer containing 100 nM TMRM [23]. In cells loaded with PG SK, loading with TMRM was started after complete dequenching with 1,10-phenanthroline (1–2 mM). The red fluorescence of TMRM excited at 543 nm with the helium/neon laser was collected through a 560–615 nm bandpass filter.

Statistics

All experiments with hepatocytes and liver endothelial cells were performed in duplicate and repeated at least three times with cells from different animals, or cells in different subcultures as appropriate. Experiments in a cell-free system were repeated at least twice. Cellular microfluorographs and traces shown in the Figures are representative of all the corresponding experiments performed. Results are expressed as means $\pm$ S.D.

RESULTS

Determination of cellular chelatable iron in cultured rat hepatocytes: general outline of the method

Hepatocellular PG SK fluorescence under baseline conditions has previously been shown to be partly quenched by the cellular chelatable iron pool [15,16]. The strong lipophilic iron chelators 2,2′-DPD or 1,10-phenanthroline added in excess to the cellular supernatant remove cellular chelatable iron from the iron-binding site of PG SK, leading to an increase in the indicator's fluorescence ('dequenching') [15,16]. In line with this, 2,2′-DPD and 1,10-phenanthroline, also under the high-resolution settings of the present study, rapidly increased intracellular PG SK fluorescence (Figures 1A, 1B, 1D, 1E and 2). As outlined previously [16], the cellular fluorescence under baseline conditions (Figures 1A and 1D) is dependent on both intracellular PG SK concentration and chelatable iron (quenching the fluorescence), whereas the fluorescence after complete dequenching (Figures 1B and 1E) is dependent only on the indicator's concentration, so the difference between the two values is dependent solely on the concentration of chelatable iron.

Cellular fluorescence of PG SK-loaded hepatocytes under baseline conditions as observed with the high spatial resolution of laser scanning microscopy (lateral resolution approx. 0.2 μm, optical slice less than 1 μm) seemed to be substantially heterogeneous before (Figures 1A and 1D) as well as after (Figures 1B and 1E) 'dequenching'. Most importantly, 'dequenching' occurred in several cellular compartments, indicating the presence of chelatable iron in these compartments. Under baseline conditions, the compartmental distribution of PG SK fluorescence as shown in Figures 1(A) and 1(D) remained constant for at least 1 h (results not shown). Surprisingly, there was a marked difference in the pattern of 'dequenching' depending on whether 2,2′-DPD (5 mM) or 1,10-phenanthroline (1–2 mM) was used for the purpose, with only the latter effectively dequenching the numerous small 'dark voids' observed under baseline conditions (Figures 1A, 1B, 1D and 1E); this suggests that some organelles have different permeabilities to the two chelators (see below). Because 1,10-phenanthroline obviously had access to subcellular compartments that were not accessible to 2,2′-DPD, the following quantitative studies on subcellular chelatable iron were performed with 1,10-phenanthroline for 'dequenching'.

The average intracellular concentration of PG SK within hepatocytes, determined from the height of the plateau after 'dequenching' with 1,10-phenanthroline (1 mM) compared with that of PG SK (free dye) standards in an *ex situ* calibration performed with the LSM 510 system as described previously [16], was 21.6 ± 7.9 μM (mean $\pm$ S.D.; $n = 5$ experiments from four different animals). The difference in cellular PG SK fluorescence between the baseline condition and the 'dequenched' condition can be used as a direct measure of the intracellular concentration of chelatable iron provided that the indicator concentration is not limiting (i.e. the concentration of PG SK has to exceed the concentration of chelatable iron at least 3-fold, permitting the formation of a 3:1 complex [16]). With the use of an *ex situ* calibration in a 'cytosolic medium' as described previously [16] we determined an average concentration of 5.0 ± 2.0 μM chelatable iron in cultured rat hepatocytes when the signals were integrated over whole cells (mean $\pm$ S.D.; $n = 5$ experiments from four different animals). In what follows, we address the different cellular compartments of cultured hepatocytes.

Intranuclear chelatable iron

PG SK fluorescence within the hepatocellular nuclei, both before and after the addition of 2,2′-DPD or 1,10-phenanthroline, was clearly higher than it was within the surrounding cytosol and the remaining compartments (Figures 1A, 1B, 1D, 1E and 2). By using the *ex situ* calibration methods described above, we determined an intranuclear PG SK concentration of 28.3 ± 9.1 μM and a surprisingly high concentration of chelatable iron, 6.6 ± 2.9 μM.

Mitochondrial chelatable iron

Under baseline conditions, individual mitochondria [identified by TMRM staining; Figures 1(C) and 1(F)] appeared as small dark round voids surrounded by cytosolic PG SK fluorescence (Figures 1A and 1D). After the addition of 2,2′-DPD (5 mM), almost no increase in mitochondrial PG SK fluorescence was detectable (Figure 1B). Because baseline fluorescence depends on both the cellular indicator concentration and the concentration of chelatable iron (see above), this indicates either that the mitochondria do not contain PG SK or that 2,2′-DPD (5 mM) does not enter the mitochondrial compartment sufficiently and therefore fails to 'dequench' the indicator. To differentiate between these two possibilities we employed the transition-metal chelator 1,10-phenanthroline (1–2 mM), which is reported to pass through the inner mitochondrial membrane. When 1,10-phenanthroline (1–2 mM) was added to PG SK-loaded hepatocytes, mitochondrial fluorescence increased within 20–40 min, indicating that hepatocellular mitochondria contained PG SK that was quenched by iron under baseline conditions (Figures 1D, 1E and 2). Thus the mitochondria seemed to contain significant amounts of chelatable iron. In cultured hepatocytes, mitochondrial PG SK-chelatable iron is thus evidently accessible to 1,10-phenanthroline (1 mM) but not to 2,2′-DPD (5 mM). Preincubation of hepatocytes with 2,2′-DPD (5 mM), 20 min before loading with PG SK was started and in the presence of PG SK, had no effect on the increase of mitochondrial PG SK fluorescence caused by 1,10-phenanthroline, indicating that no chelatable iron was transferred from the cytosol into mitochondria during PG SK loading. 1,10-Phenanthroline (1–2 mM)

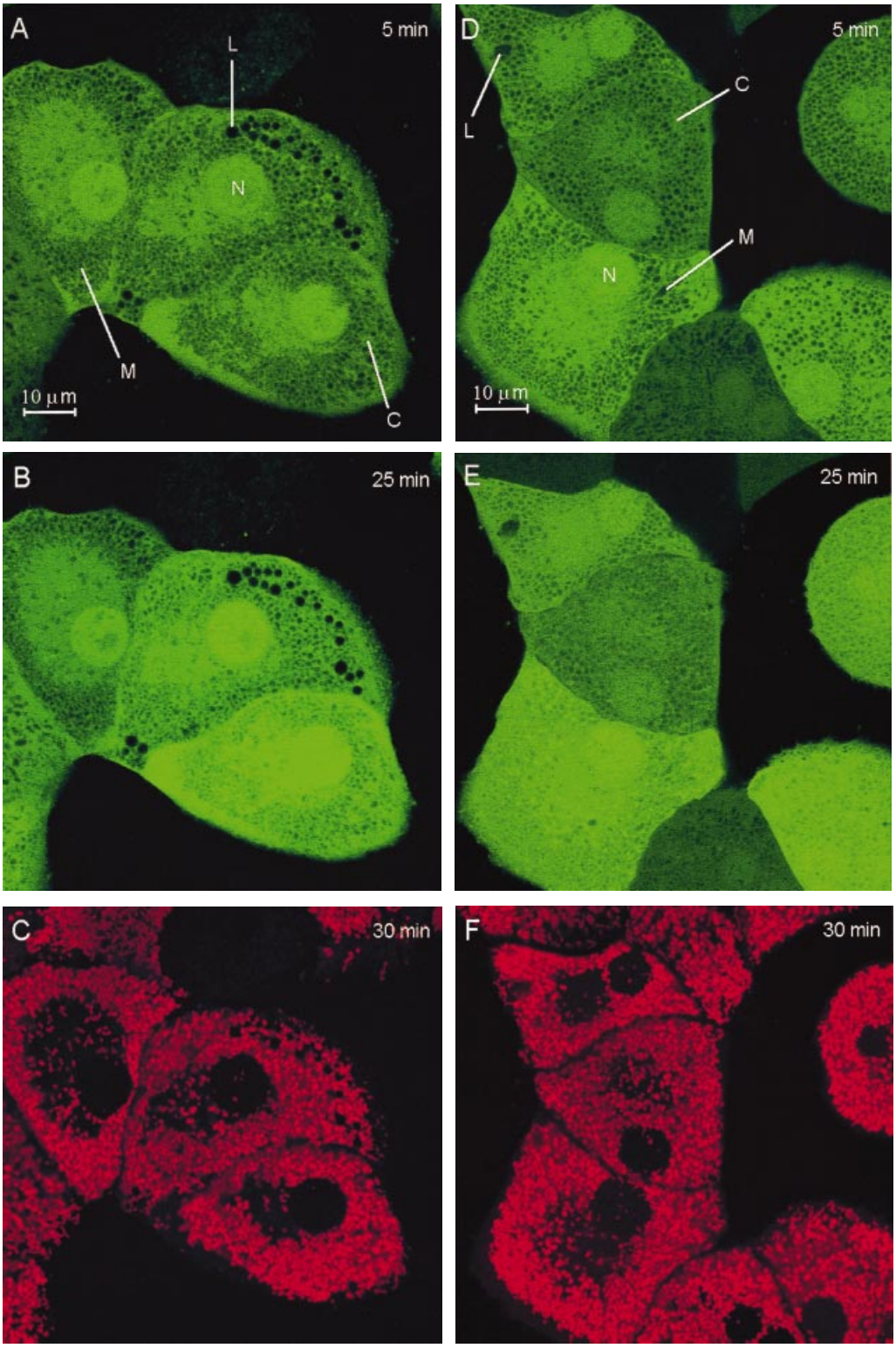

Figure 1 'Dequenching' of the subcellular fluorescence of PG SK-loaded cultured hepatocytes by the addition of membrane-permeant transition-metal chelators

The cells were loaded with the diacetate of PG SK for 10 min in HBSS (at 37 °C) and then incubated in Krebs–Henseleit buffer. Subcellular fluorescence of PG SK was imaged with laser scanning microscopy ($\lambda_{excitation} = 488$ nm; $\lambda_{emission} \geqslant 505$ nm). After establishment of the baseline fluorescence (5 min), images were collected before (**A**, **D**) and after (**B**, **E**) addition of the transition-metal chelators 2,2′-DPD (5 mM) (**A**, **B**) or 1,10-phenanthroline (2 mM) (**D**, **E**), detecting baseline fluorescence (**A**, **D**) and fluorescence after complete equilibration after addition of the chelators (**B**, **E**) (compare with Figure 2). After 'dequenching' of the cellular PG SK fluorescence, TMRM (1 μM) was added to the supernatant to stain intact mitochondria; red TMRM fluorescence ($\lambda_{excitation} = 543$ nm; $\lambda_{emission} = 560$–615 nm) was imaged 5 min later (**C**, **F**). Abbreviations: C, cytosol; L, lipid vesicles; M, mitochondria; N, nucleus.

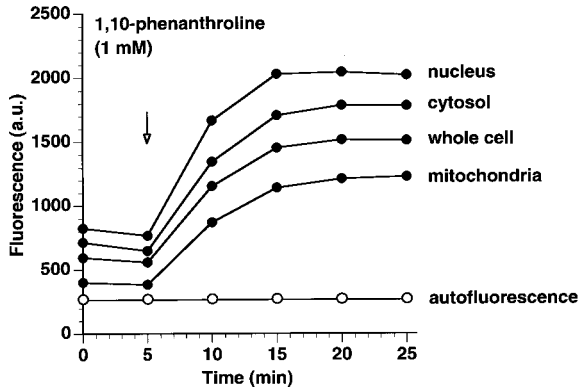

Figure 2 Quantitative determination of the increase in subcellular PG SK fluorescence of cultured rat hepatocytes after the addition of 1,10-phenanthroline (1 mM)

Cells were cultured on glass coverslips and loaded with PG SK by incubation at 37 °C with the diacetate form (20 μM) for 10 min in HBSS. After establishment of the baseline fluorescence, intracellular PG SK fluorescence was 'dequenched' by the addition of excess 1,10-phenanthroline (1 mM) (indicated by the arrow) to obtain the maximum signal (i.e. no fluorescence quenching). Subcellular fluorescence [in arbitrary units (a.u.)] within hepatocellular compartments was recorded at 5 min intervals by using quantitative laser scanning microscopy ($\lambda_{excitation} = 488$ nm; $\lambda_{emission} \geqslant 505$ nm). Each trace shown is the average of data obtained from three cells and is representative of five experiments with cells from different animals.

had no effect on mitochondrial integrity or mitochondrial membrane potential (Figure 1F); TMRM labelling of mitochondria did not decrease over a period of 1 h after the addition of 2 mM 1,10-phenanthroline (results not shown).

The intramitochondrial concentration of PG SK was 18.2 ± 8.7 μM. The concentration of the mitochondrial chelatable iron pool amounted to at least 4.8 ± 2.3 μM. Under baseline conditions, intramitochondrial PG SK fluorescence was practically completely quenched ('dark voids'; Figures 1D and 2); the remaining fluorescence equalled 3.3 ± 2.4 μM unquenched PG SK. Therefore we cannot exclude the possibility that PG SK was locally limiting (for details see [16]) and the concentration of mitochondrial chelatable iron given above has to be regarded as a minimum.

To further exclude a redistribution of PG SK from the cytosol into the mitochondria or a displacement of cytosolic iron into the mitochondria, we assessed chelatable iron in mitochondria of permeabilized hepatocytes. When 1,10-phenanthroline (2 mM) was added to cells that had been loaded with PG SK and subsequently permeabilized with digitonin, the mitochondrial fluorescence intensity increased substantially (results not shown), confirming the existence of a pool of mitochondrial chelatable iron. The concentration of mitochondrial chelatable iron as determined in permeabilized hepatocytes was 1.5 ± 0.7 μM. This concentration is substantially lower than that determined in mitochondria of intact cells; however, it is likely that the value obtained in permeabilized cells is markedly underestimated because cell permeabilization resulted in mitochondrial swelling (and thus dilution of both the iron and the indicator).

Cytosolic chelatable iron pool

The cytosol of PG SK-loaded hepatocytes seemed to be diffusely labelled with the indicator. Dark round voids in the cytosolic PG SK fluorescence were identified as mitochondria (see above) and as lipid vesicles (see below); the endoplasmic reticulum appeared as a mitochondria-free fluorescent area near the nucleus (Figures 1A and 1D). The cytosol, as defined for the measurements, is the 'structureless' space between mitochondria. The addition of 1,10-phenanthroline (1 mM) increased PG SK fluorescence in this space in a way that corresponded to an indicator concentration of 24.6 ± 9.6 μM (Figures 1D, 1E and 2) and a concentration of cytosolic chelatable iron of 5.0 ± 2.0 μM.

Chelatable iron in other subcellular compartments

The large dark voids, not dequenched under any conditions and therefore probably not containing PG SK, correspond to lipid vesicles as assessed by labelling with Sudan II (results not shown). Unfortunately, it was not possible to determine chelatable iron in lysosomes for several reasons: lysosomes make up only 1.1 % of the total hepatocellular volume and are extremely small [24]. Individual lysosomes within the surrounding cytosolic PG SK fluorescence were detectable only after being labelled with Acridine Orange, a lysosomotropic, weak base that accumulates in lysosomes and emits pH-dependent fluorescence. However, double staining with Acridine Orange and PG SK was not possible because the strong Acridine Orange signal overlapped the PG SK signal. It was not possible to back-track the small lysosomes invisible before 'dequenching' and identified with Acridine Orange after 'dequenching' to previous images, owing to the movements of all organelles in the viable cells used in this study (this was corrected for in all measurements described above by re-adjusting the position of the areas in which fluorescence was quantified).

Possible confounding factors

When hepatocytes were incubated with PG SK pre-complexed to Fe^{2+} (molar ratio 2:1), the cellular PG SK fluorescence after completely dequenching, i.e. after the addition of 1,10-phenthroline (1 mM) was less than 10 % of that in cells loaded with PG SK substantially free from contaminant iron (results not shown). This suggests that the PG SK/Fe^{2+} complex is almost membrane-impermeant, which could be expected because the molecular mass of the complex is high and the lipophilicity of other bidentate chelators has been found to decrease when forming a complex with iron [25,26]. Therefore it is most unlikely that contaminant iron from the buffer was loaded into cells by the indicator; this was confirmed by another control with PG SK preincubated with the Fe^{3+} chelator diethylenetriaminepentaacetic acid (200 μM): in the absence of any contaminant iron, the indicator provided the same increase in fluorescence as that used under standard conditions. Given the evidently low membrane permeability of the PG SK/Fe^{2+} complex, the risk that PG SK might transfer chelatable iron from a subcellular compartment into another during dye loading should also be a minor one.

PG SK fluorescence and its Fe^{2+}-induced quenching are largely unaffected by possible environmental variations within cells, such as ionic strength and viscosity [15], or organic iron chelators (e.g. citrate, phosphate and ATP) [16]. There was no effect of pH on either PG SK fluorescence or Fe^{2+}-induced quenching over a wide pH range (pH 6.2–8.5); however, below pH 6.2 the PG SK fluorescence gradually decreased and was practically absent below pH 5.0. Therefore, determining chelatable iron after calibration *ex situ* in a medium that simulates the composition of the cytosol is also permissible for the other subcellular compartments except for lysosomes, although environmental conditions within these compartments are not 'cytosolic'.

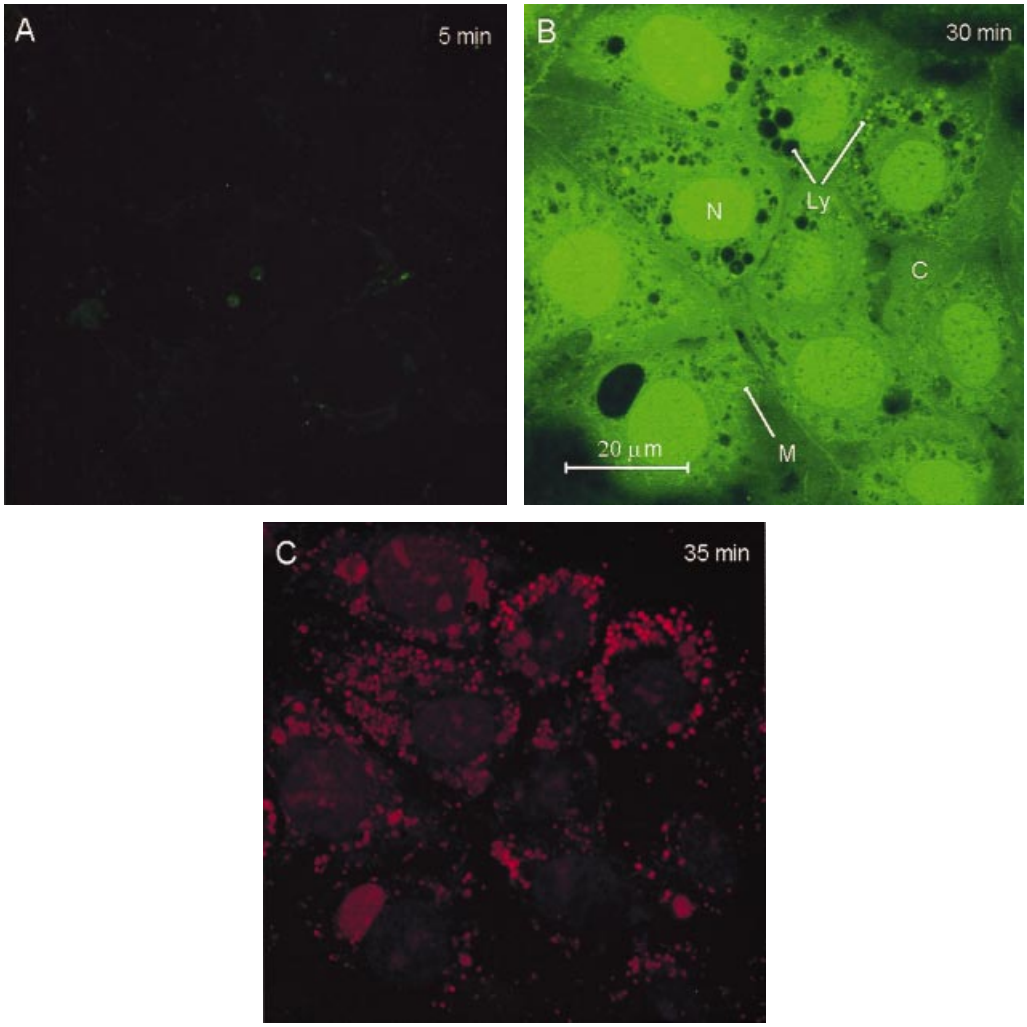

Figure 3 Subcellular distribution of chelatable iron in liver endothelial cells

Liver endothelial cells were loaded with PG SK by incubation at 37 °C with the diacetate form (20 μM) for 30 min in HBSS. After establishment of the baseline fluorescence (**A**), chelatable iron was removed from the intracellular indicator by the addition of excess 1,10-phenanthroline (2 mM) to obtain the maximum signal (**B**) (compare with Figure 1E). After the 'dequenching' of the cellular PG SK fluorescence, Acridine Orange (0.5 μg/ml) was added to the supernatant to stain intact lysosomes (**C**). Acridine Orange fluorescence ($\lambda_{excitation} = 488$ nm; $\lambda_{emission} \geqslant 560$ nm) was imaged 5 min later. Abbreviations: C, cytosol; Ly, lysosomes/endosomes; M, mitochondria; N, nucleus.

Subcellular distribution of chelatable iron in liver endothelial cells

For purposes of comparison we assessed the subcellular distribution of chelatable iron in a second cell type, namely liver endothelial cells, which we chose especially because of their numerous and large lysosomes [24]. The cellular fluorescence of PG SK-loaded liver endothelial cells under baseline conditions hardly exceeded autofluorescence (Figure 3A). 1,10-Phenanthroline (2 mM), added to endothelial cells loaded with PG SK, increased cellular fluorescence by far more than in hepatocytes, indicating higher concentrations of chelatable iron. An increase in fluorescence was detectable within the nuclei, in the cytosol and within mitochondria, but only within some of the endosomes/lysosomes (Figure 3). The latter could be an effect of the intralysosomal low pH; however, when the lysosomal pH of PG SK-loaded endothelial cells was increased by adding the lysosomotropic weak base methylamine (40 mM) [27] after 'dequenching' with 2 mM 1,10-phenanthroline, the non-fluorescent lysosomes remained non-fluorescent (and the fluorescence of the PG SK-containing lysosomes did not increase). Thus, only a subpopulation of the endosomal/lysosomal apparatus could be loaded with PG SK. This subpopulation, which consisted predominantly of small endosomes/lysosomes (and which, with regard to the inability of methylamine to increase the PG SK fluorescence within these organelles, possibly had a relatively high pH) did contain chelatable iron, whereas for the other subpopulations this question remains open.

The kinetics of the increases in fluorescence was almost the same in the various subcellular compartments of endothelial cells but the magnitude of the increases differed markedly, indicating different concentrations of chelatable iron within these compartments. Using the *ex situ* calibration procedure described above, we determined an average concentration of chelatable iron within rat liver endothelial cells of 8.0 ± 2.7 μM. As we found for hepatocytes, the endothelial cells' nuclei also contained a surprisingly high concentration of chelatable iron of 11.8 ± 3.9 μM. In endothelial cells, the concentration of chelatable iron within mitochondria was even higher (9.2 ± 2.7 μM) than within the

cytosol (7.3 ± 2.6 μM; means $\pm$ S.D. from $n = 4$ independent experiments) and, in contrast to hepatocytes, endothelial mitochondria were also 'dequenched' by 2,2′-DPD (5 mM; results not shown). Chelatable iron within the PG SK-stained subpopulation of the endosomal/lysosomal apparatus was 15.8 ± 4.1 μM, when calibration was performed at pH 6.0; performing calibration at lower pH values would yield even higher iron concentrations (pH 6.0, at the upper limit of pH values in the endosomal/lysosomal apparatus, was used for calibration to avoid any overestimation of the values obtained in this small subpopulation, the pH of which is unknown). Owing to the small number of these PG SK-stained organelles (in comparison with the whole number of endosomes/lysosomes) per cell and owing to the pH dependence of PG SK fluorescence, the value given has to be viewed with caution; however, the results clearly indicate that at least a subpopulation of endosomes/lysosomes contains a very high concentration of chelatable iron.

DISCUSSION

The present study explores the distribution of chelatable iron in viable rat liver cells. We showed, in cultured rat hepatocytes and rat liver endothelial cells, that chelatable iron is distributed over several cellular compartments including the nucleus, the cytosol, lysosomes and mitochondria. The method used is the first that makes it possible to detect chelatable iron in different subcellular compartments in living cells at the single cell level.

Cellular chelatable iron is reported to belong almost exclusively to a cytosolic, so-called labile iron pool [2–5]. This pool has traditionally been studied by using cell-disruptive methods that bear the risk of artificially increasing the chelatable iron pool (e.g. by proteolysis) during the required processing of the biological samples (cell lysis or homogenization) [15]. The values obtained for chelatable iron in liver tissue and cultured hepatocytes by using cell-disruptive methods range from 3.5 to 230 μM [13,28–30], obviously reflecting the methodological difficulty in differentiating precisely between chelatable and tightly protein-bound iron ions. Furthermore, all of these methods (i.e. disruptive methods and ESR) share the drawback that they do not allow any differentiation between cytosolic chelatable and cellular chelatable iron. The cytosolic chelatable iron pool was first studied selectively in erythroleukaemia K562 cells by using the transition-metal indicator calcein acetoxymethyl ester [4]. The concentration of cytosolic chelatable iron in cultured rat liver cells as determined in the present study with PG SK (5.0 ± 2.0 μM in hepatocytes and 7.3 ± 2.6 μM in liver endothelial cells) differs markedly from the values determined in resting erythroid and myeloid cells (0.2–1.5 μM) with the calcein method [5], owing to differences between the cell types as well as between the methods (e.g. competition of calcein, but not PG SK, with organic chelators) [4,16]. Furthermore, in hepatocytes the calcein method was suitable only for assessing chelatable iron in relative terms, as calibration *in situ* was not possible [15]. However, the main drawback of the calcein method with regard to the subcellular distribution of chelatable iron is that calcein (at 37 °C) exclusively labels the hepatocellular cytosol and the nucleus [23] and therefore cannot be used to determine chelatable iron in other subcellular compartments such as the mitochondria.

Mitochondria are known to be the main source of cellular reactive oxygen species ($O_2^{-\bullet}$, H_2O_2). However, they are the site of assemblage of several iron-containing proteins and iron is incorporated into protoporphyrin IX to yield haem within the mitochondrial matrix; these processes require a mitochondrial 'transition' pool of chelatable iron. Furthermore, mitochondrial chelatable (redox-active) iron has been considered to be involved in the pathogenesis of various cytotoxic conditions and human diseases such as gentamicin toxicity [31], Friedreich's ataxia [7,32,33] and neurodegenerative diseases (such as Parkinson's and Alzheimer's diseases). Furthermore, aging [34] seems to be associated with oxidative damage to mitochondrial DNA [32,35].

Although of high physiological and pathobiochemical interest, mitochondrial chelatable iron has not yet been determined in intact cells, to the best of our knowledge. Previously, a colorimetric method was established for the determination of chelatable iron in isolated, osmotically preswollen rat liver mitochondria by using prolonged (3 h) incubation of the mitochondria with the hydrophilic transition-metal chelator bathophenanthroline sulphonate (50 μM) [8]. In another study, the desferrioxamine-available iron pool of isolated mitochondria in suspension was measured by ESR spectroscopy [6]. Methods based on (mechanical) isolation procedures, prolonged incubation with chelators and disruption of intramitochondrial structures (by preswelling) might have the inherent danger of artificially increasing the mitochondrial chelatable iron pool. These problems might be reflected by the high concentrations of chelatable iron obtained in isolated liver mitochondria: 1.7 ± 0.3 nmol/mg of mitochondrial protein [9] (approx. 330 ± 60 μM) and 0.29 ± 0.04 nmol/mg of mitochondrial protein [6] (approx. 50–60 μM; assuming that approx. 7.2×10^9 rat liver mitochondria contain 1 mg of protein and that the volume of a single mitochondrion is 0.71 μm^3) [36].

As non-invasive fluorescence microscopy uses living cells, disturbance from any pretreatment of biological samples (such as organelle isolation) is minimized [15] but the concentration of mitochondrial chelatable iron as determined in the present study (cultured rat hepatocytes, 4.8 ± 2.3 μM; liver endothelial cells, 9.2 ± 2.7 μM) has to be regarded as a lower limit because intramitochondrial PG SK fluorescence was practically quenched completely under baseline conditions (see the Results section). It is still a drawback of our method that subcellular PG SK concentrations as obtained during loading of the cells with the diacetate form of the indicator do not sufficiently (more than 3-fold) exceed the concentration of chelatable iron in all compartments to ensure complete formation of the indicator(3)/Fe^{2+}(1) complex [16]. However, this is a problem that should be amenable to modifications of the indicator molecule in the future.

Surprisingly, in contrast with PG SK fluorescence in liver endothelial cells, mitochondrial PG SK fluorescence of cultured rat hepatocytes could not be 'dequenched' by 2,2′-DPD (5 mM). There are three particularly important factors on which the 'dequenching' of PG SK fluorescence after a redistribution of iron from the fluorescent indicator to a chelator largely depends: one is the chelator's iron-binding constant for Fe^{2+}, another is the chelator's ability to enter subcellular compartments (i.e. its subcellular distribution), and a third is its subcellular concentration (which is a function of a molecule's charge, size and lipophilicity) [26,37]. The most likely explanation is that in hepatocytes 2,2′-DPD cannot pass the inner mitochondrial membrane sufficiently well, suggesting differences in membrane structure; however, the effect of this might be aggravated by surface-to-volume ratios (more spherical mitochondria in hepatocytes and filamentous mitochondria in endothelial cells) (Figures 1C and 3B).

Oxidative DNA damage is considered to be an important step in the pathogenesis of human diseases such as cancer and is believed to be mediated by highly redox-active DNA-associated iron [1,2]. To our knowledge, the existence of nuclear iron that is chelatable has not been demonstrated until now. The surprisingly high concentrations of nuclear chelatable iron de-

termined here (cultured rat hepatocytes, $6.6 \pm 2.9\ \mu M$; liver endothelial cells, $11.8 \pm 3.9\ \mu M$) clearly exceed the cytosolic chelatable iron pool (see above) and might reflect an extensive intranuclear iron metabolism: nuclear ferritin was found in nuclei of corneal epithelial cells [38] and in nuclei of liver cells [39]; the total concentration of iron in the nucleus is reported to be similar to [40] or even larger than the cytosolic iron concentration [1,41]. Although low-molecular-mass species, including metal ions, have previously been considered to be freely diffusible across the nuclear pores, more recently an active (ATPase-driven) transportation of Ca^{2+} [42] and Fe^{3+} [43] into isolated rat liver nuclei has been described and cell nuclei therefore have to be regarded as separate metabolic compartments.

Lysosomes have been reported to contain high concentrations of iron in transit (owing to intralysosomal degradation of metalloproteins) [44] which is thought by some groups to constitute an important pool catalysing the decomposition of H_2O_2, yielding the highly reactive hydroxyl radical [10,11]. Intralysosomal iron has been reported to increase under pathological conditions such as oxidative stress [12], nutrient deprivation [13] and in several models of renal diseases [14]; such iron is therefore considered to contribute to various diseases. However, it seems unclear, given the methods used in the above studies, whether chelatable or total intralysosomal iron was determined. Using the present method we determined chelatable iron within a subpopulation of the endosomal/lysosomal apparatus of rat liver endothelial cells. It is not yet known why PG SK enters only some of these organelles, and the pH sensitivity of PG SK (i.e. the pH sensitivity of the fluorophor fluorescein) is clearly compromising the use of this indicator in these acidic organelles. However, the results show that in principle the detection of lysosomal chelatable iron is possible with our method and suggest that the lysosomal/endosomal pool might be surprisingly high. Improved indicators are therefore currently being designed to achieve higher lysosomal concentrations of indicators with pH-independent fluorescence.

Taken together, our results indicate clearly that chelatable iron in intact liver cells is not restricted to a cytosolic pool, as is generally described, but is also present in various other subcellular compartments, suggesting a metabolic compartmentation of intracellular iron. This could be shown in primary cells as well as in a cell line. Although the cultured hepatocytes as used in the present study (24 h after cell isolation) had a total iron content that did not differ from freshly isolated cells, the total iron content of the liver endothelial cells studied was decreased even when compared with freshly isolated liver endothelial cells (F. Petrat, H. de Groot and U. Rauen, unpublished work). The latter finding, which is in line with published results (in which some degree of iron depletion is well known for cell lines [45]), renders the high level of chelatable iron observed in the different compartments of the liver endothelial cells even more surprising.

The identification of several subcellular chelatable iron pools in the present study should be important under pro-oxidant conditions, in which these iron pools might have the potential to catalyse the generation of hydroxyl radicals leading to oxidative cell damage in the respective compartment. In particular, the mitochondrial chelatable iron pool (i.e. chelatable iron localized at a site of high $O_2^{-\bullet}/H_2O_2$ production) and the surprisingly high concentration of chelatable iron in cell nuclei (with the associated risk of DNA damage) are of great pathophysiological interest. Knowledge of the subcellular distribution of iron as well as of the iron chelators employed is important when iron chelators are used for cellular protection under oxidative stress. The method presented permits the study of the distribution of both iron and chelator and should therefore be useful in assessing the contribution of chelatable iron to pathological conditions and diseases. Furthermore, the method should permit on-line measurements of iron uptake into cellular compartments, a feature that is of high interest in the light of the recent identification of specific transporters for iron in intracellular membranes [33,43]. Further improvement is to be expected when different fluorescent iron indicators become available that can be selectively (and sufficiently) loaded into a particular subcellular compartment.

We thank Mrs E. Hillen, Ms B. Büchner and Mrs M. Brachvogel for their technical assistance in the isolation and cultivation of the cells, and Mr H. Diederichs (Institut für Arbeitsmedizin, Universitätsklinikum Essen) for the AAS measurements. This work was supported by a grant from the Medical Faculty of the University of Essen (IFORES-Programm).

REFERENCES

1 Meneghini, R. (1997) Iron homeostasis, oxidative stress, and DNA damage. Free Radical Biol. Med. **23**, 783–792
2 Halliwell, B. and Gutteridge, J. M. C. (1990) Role of free radicals and catalytic metal ions in human disease: an overview. Methods Enzymol. **186**, 1–85
3 Young, S. P. and Aisen, P. (1994) The liver and iron. In The Liver: Biology and Pathobiology (Arias, I. M., Boyler, J. L. and Fausto, N., eds.), pp. 597–617, Raven Press, New York
4 Breuer, W., Epsztejn, S. and Cabantchik, Z. I. (1995) Iron acquired from transferrin by K562 cells is delivered into a cytoplasmic pool of chelatable iron(II). J. Biol. Chem. **270**, 24209–24215
5 Epsztejn, S., Kakhlon, O., Glickstein, H., Breuer, W. and Cabantchik, Z. I. (1997) Fluorescence analysis of the labile iron pool of mammalian cells. Anal. Biochem. **248**, 31–40
6 Ceccarelli, D., Gallesi, D., Giovannini, F., Ferrali, M. and Masini, A. (1995) Relationship between free iron level and rat liver mitochondrial dysfunction in experimental dietary iron overload. Biochem. Biophys. Res. Commun. **209**, 53–59
7 Foury, F. and Cazzalini, O. (1997) Deletion of the yeast homologue of the human gene associated with Friedreich's ataxia elicits iron accumulation in mitochondria. FEBS Lett. **411**, 373–377
8 Flatmark, T. and Tangeras, A. (1976) Mitochondrial 'non-heme non-FeS iron' and its significance in the cellular metabolism of iron. In Proteins of Iron Metabolism (Brown, E. B., Aisen, P., Fielding, J. and Crichton, R. R., eds.), pp. 349–358, Grune & Stratton, New York
9 Tangeras, A., Flatmark, T., Bäckström, D. and Ehrenberg, A. (1980) Mitochondrial iron not bound in heme and iron–sulfur centers. Estimation, compartmentation and redox state. Biochim. Biophys. Acta **589**, 162–175
10 Brunk, U. T., Zhang, H., Roberg, K. and Öllinger, K. (1995) Lethal hydrogen peroxide toxicity involves lysosomal iron-catalyzed reactions with membrane damage. Redox Report **1**, 267–277
11 Nilsson, E., Ghassemifar, R. and Brunk, U. T. (1997) Lysosomal heterogeneity between and within cells with respect to resistance against oxidative stress. Histochem. J. **29**, 857–865
12 Öllinger, K. and Brunk, U. T. (1995) Cellular injury induced by oxidative stress is mediated through lysosomal damage. Free Radical Biol. Med. **19**, 565–574
13 Öllinger, K. and Roberg, K. (1997) Nutrient deprivation of cultured rat hepatocytes increases the desferrioxamine-available iron pool and augments the sensitivity to hydrogen peroxide. J. Biol. Chem. **272**, 23707–23711
14 Nankivell, B. J., Tay, Y.-C., Boadle, R. A. and Harris, D. C. H. (1994) Dietary protein alters tubular iron accumulation after partial nephrectomy. Kidney Int. **45**, 1006–1013
15 Petrat, F., Rauen, U. and de Groot, H. (1999) Determination of the chelatable iron pool of isolated rat hepatocytes by digital fluorescence microscopy using the fluorescent probe, phen green SK. Hepatology **29**, 1171–1179
16 Petrat, F., de Groot, H. and Rauen, U. (2000) Determination of the chelatable iron pool of single intact cells by laser scanning microscopy. Arch. Biochem. Biophys. **376**, 74–81
17 de Groot, H. and Brecht, M. (1991) Reoxygenation injury in rat hepatocytes: mediation by O_2^-/H_2O_2 liberated by sources other than xanthine oxidase. Biol. Chem. Hoppe-Seyler **372**, 35–41
18 Rauen, U., Hanssen, M., Lauchart, W., Becker, H. D. and de Groot, H. (1993) Energy-dependent injury to cultured sinusoidal endothelial cells of the rat liver in UW solution. Transplantation **55**, 469–473
19 Rauen, U., Polzar, B., Stephan, H., Mannherz, H. G. and de Groot, H. (1999) Cold-induced apoptosis in cultured hepatocytes and liver endothelial cells: mediation by reactive oxygen species. FASEB J. **13**, 155–168

20 Romeis, B. (1989) Mikroskopische Technik, Verlag Urban & Schwarzenberg, Munich
21 Taylor, D. E., Ghio, A. J. and Piantadosi, C. A. (1995) Reactive oxygen species produced by liver mitochondria of rats in sepsis. Arch. Biochem. Biophys. **316**, 70–76
22 Pastorino, J. G., Snyder, J. W., Hoek, J. B. and Farber, J. L. (1995) Ca^{2+} depletion prevents anoxic death of hepatocytes by inhibiting mitochondrial permeability transition. Am. J. Physiol. **268**, C676–C685
23 Zahrebelski, G., Nieminen, A.-L., Al-Ghoul, K., Qian, T., Herman, B. and Lemasters, J. J. (1995) Progression of subcellular changes during chemical hypoxia to cultured rat hepatocytes: a laser scanning confocal microscopic study. Hepatology **21**, 1361–1372
24 Blouin, A., Bolender, R. P. and Weibel, E. R. (1977) Distribution of organelles and membranes between hepatocytes and nonhepatocytes in the rat liver parenchyma. J. Cell Biol. **72**, 441–455
25 Hershko, C., Link, G., Pinson, A., Peter, H. H., Dobbin, P. and Hider, R. C. (1991) Iron mobilization from myocardial cells by 3-hydroxypyridin-4-one chelators: studies in rat heart cells in culture. Blood **77**, 2049–2053
26 Porter, J. B., Gyparaki, M., Burke, L. C., Huehns, E. R., Sarpong, P., Saez, V. and Hider, R. C. (1988) Iron mobilization from hepatocyte monolayer cultures by chelators: the importance of membrane permeability and the iron-binding constant. Blood **72**, 1497–1503
27 Myers, B. M., Tietz, P. S., Tarara, J. E. and LaRusso, N. F. (1995) Dynamic measurements of the acute and chronic effects of lysosomotropic agents on hepatocyte lysosomal pH using flow cytometry. Hepatology **22**, 1519–1526
28 Baliga, R., Ueda, N. and Shah, S. V. (1993) Increase in bleomycin-detectable iron in ischaemia/reperfusion injury to rat kidneys. Biochem. J. **291**, 901–905
29 Cairo, G., Tacchini, L., Pogliaghi, G., Anzon, E., Tomasi, A. and Bernelli-Zazzera, A. (1995) Induction of ferritin synthesis by oxidative stress. Transcriptional and post-transcriptional regulation by expansion of the 'free' iron pool. J. Biol. Chem. **270**, 700–703
30 Nielsen, P., Düllmann, J., Wulfhekel, U. and Heinrich, H. C. (1993) Non-transferrin-bound-iron in serum and low-molecular-weight-iron in the liver of dietary iron-loaded rats. Int. J. Biochem. **25**, 223–232
31 Ueda, N., Guidet, B. and Shah, S. V. (1993) Gentamicin-induced mobilization of iron from renal cortical mitochondria. Am. J. Physiol. **265**, F435–F439
32 Beal, M. F. (1998) Mitochondrial dysfunction in neurodegenerative diseases. Biochim. Biophys. Acta **1366**, 211–223
33 Askwith, C. and Kaplan, J. (1998) Iron and copper transport in yeast and its relevance to human disease. Trends Biochem. Sci. **23**, 135–138
34 Johnson, F. B., Sinclair, D. A. and Guarente, L. (1999) Molecular biology of aging. Cell **96**, 291–302
35 Ozawa, T., Hayakawa, M., Katsumata, K., Yoneda, M., Ikebe, S. and Mizuno, Y. (1997) Fragile mitochondrial DNA: The missing link in the apoptotic neuronal cell death in Parkinson's disease. Biochem. Biophys. Res. Commun. **235**, 158–161
36 Tyler, D. D. (1992) The Mitochondrion in Health and Disease, VCH Publishers, New York
37 Lytton, S. D., Mester, B., Dayan, I., Glickstein, H., Libman, J., Shanzer, A. and Cabantchik, Z. I. (1993) Mode of action of iron(III) chelators as antimalarials: I. Membrane permeation properties and cytotoxic activity. Blood **81**, 214–221
38 Cai, C. X., Birk, D. E. and Linsenmayer, T. F. (1998) Nuclear ferritin protects DNA from UV damage in corneal epithelial cells. Mol. Biol. Cell. **9**, 1037–1051
39 Smith, A. G., Carthew, P., Francis, J. E., Edwards, R. E. and Dinsdale, D. (1990) Characterization and accumulation of ferritin in hepatocyte nuclei of mice with iron overload. Hepatology **12**, 1399–1405
40 Lai, C. C., Huang, W. H., Klevay, L. M., Gunning, III, W. T. and Chiu, T. H. (1996) Antioxidant enzyme gene transcription in copper-deficient rat liver. Free Radical Biol. Med. **21**, 233–240
41 Csermely, P., Fodor, P. and Somogyi, J. (1987) The tumor promotor tetradecanoylphorbol-13-acetate elicits the redistribution of heavy metals in subcellular fractions of rabbit thymocytes as measured by plasma emission spectroscopy. Carcinogenesis **8**, 1663–1666
42 Nicotera, P., Zhivotovsky, B. and Orrenius, S. (1994) Nuclear calcium transport and the role of calcium in apoptosis. Cell Calcium **16**, 279–288
43 Gurgueira, S. A. and Meneghini, R. (1996) An ATP-dependent iron transport system in isolated rat liver nuclei. J. Biol. Chem. **271**, 13616–13620
44 von Zglinicki, T. and Brunk, U. T. (1993) Intracellular interactions under oxidative stress and aging: a hypothesis. Z. Gerontol. **26**, 215–220
45 Recalcati, S., Conte, D. and Cairo, G. (1999) Preferential activation of iron regulatory protein-2 in cell lines as a result of higher sensitivity to iron. Eur. J. Biochem. **259**, 304–309

Received 7 September 2000/1 November 2000; accepted 22 February 2001